PHYSICAL REVIEW D **87,** 074006 (2013)

Confirming the molecular nature of the $Z_b(10610)$ and the $Z_b(10650)$

Martin Cleven,[1,*] Qian Wang,[1,†] Feng-Kun Guo,[2,‡] Christoph Hanhart,[1,3,§] Ulf-G. Meißner,[1,2,3,‖] and Qiang Zhao[4,¶]

[1]*Institut für Kernphysik Jülich Center for Hadron Physics, Forschungszentrum Jülich, D-52425 Jülich, Germany*

[2]*Helmholtz-Institut für Strahlen- und Kernphysik Bethe Center for Theoretical Physics, Universität Bonn, D-53115 Bonn, Germany*

[3]*Institute for Advanced Simulation, Forschungszentrum, Jülich, D-52425 Jülich, Germany*

[4]*Institute of High Energy Physics Theoretical Physics Center for Science Facilities, Chinese Academy of Sciences, Beijing 100049, China*

(Received 5 February 2013; published 9 April 2013)

The decays of the $Z_b(10610)$ and the $Z_b(10650)$ to $\Upsilon(nS)\pi$, $h_b(mP)\pi$ and $\chi_{bJ}(mP)\gamma$ ($n = 1, 2, 3$, $m = 1, 2$ and $J = 0, 1, 2$) are investigated within a nonrelativistic effective field theory. It is argued that, while the decays to $\Upsilon(nS)\pi$ suffer from potentially large higher order corrections, the P-wave transitions of the Z_b states are dominated by a single one-loop diagram and therefore offer the best possibility to confirm the nature of the Z_b states as molecular states and to further study their properties. We give nontrivial and parameter-free predictions for the ratios of various partial widths of the Z_b and Z_b' into final states with $h_b(mP)\pi$ and $\chi_{bJ}(mP)\gamma$. While such relations appear naturally in the molecular picture for the mentioned transitions, they are not expected to hold for any other scenario. In addition, the branching fractions for the neutral Z_b states to $\chi_{bJ}\gamma$ are predicted to be of order 10^{-4}–10^{-3}. This provides a fine test of the molecular nature in future high-luminosity experiments.

DOI: 10.1103/PhysRevD.87.074006 PACS numbers: 12.39.Hg, 14.40.Rt, 13.25.Jx

I. INTRODUCTION

Recently the Belle Collaboration found two narrow structures, namely the $Z_b(10610) = Z_b^{\pm}$ and the $Z_b'(10650) = Z_b'^{\pm}$, in the $\Upsilon(nS)\pi^{\pm}$ ($n = 1, 2, 3$) and $h_b(mP)\pi^{\pm}$ ($m = 1, 2$) invariant masses of the $\Upsilon(5S) \to \Upsilon(nS)\pi^+\pi^-$ and $\Upsilon(5S) \to h_b(mP)\pi^+\pi^-$ decay processes [1]. In their latest data, the open-bottom channels $B^*\bar{B}$ and $B^*\bar{B}^*$ are also seen [2]. The fact that they lie in the bottomonium mass region and they are charged means that they cannot be the conventional bottomonium mesons, and their isospins are 1. The observation of the neutral state with a mass consistent with that of the $Z_b(10610)$ [3] presents a further confirmation that they are members of isotriplets. If they exist as observed by the Belle Collaboration, they must be exotic states with a pair of hidden $b\bar{b}$ and valence light quarks. Considering parity and charge parity, their quantum numbers should be $I^G(J^P) = 1^+(1^+)$, and the charge parity of the neutral state is negative.

Assuming that the total width of $Z_b^{(\prime)}$ is saturated by the seven channels already observed experimentally, i.e., $\Upsilon(nS)\pi$ ($n = 1, 2, 3$), $h_b(mP)\pi (m = 1, 2)$, $B\bar{B}^* + B^*\bar{B}$ and $B^*\bar{B}^*$, Belle gives the branching ratio of each channel in $\Upsilon(5S)$ three-body decays [2]. The proximity of the states to the $B^{(*)}\bar{B}^*$ thresholds leads to the suggestion that they could be hadronic molecules of the corresponding states [4–12], to be distinguished from the compact $\bar{b}\,\bar{q}\,bq$ tetraquarks [11,13,14]. By hadronic molecules, we mean states composed of hadrons—they can be bound states (poles on the physical sheet with respect to the bottom-meson channel with a mass smaller than the threshold value), resonances or virtual states (both on the second sheet with respect to the relevant bottom-meson channel—the former above, the latter below the threshold). Based on a nonrelativistic effective field theory (NREFT) [15,16], the authors of Ref. [5] show that the $h_b(1P, 2P)\pi^{\pm}$ data can be described within the bound state scenario. Therein, the $Z_b^{(\prime)}B^{(*)}\bar{B}^*$ coupling constants are related to the binding energies using a model-independent relation for S-wave shallow bound states [17,18]. However, since data on the decays of $Z_b^{(\prime)}$ to open-bottom channels are now available, we can choose a more general ansatz and take these couplings from data directly—in this way our results are valid for bound states, resonances and virtual states. Since we start from the assumption that the Z_b states are purely molecular states, their decays into the $\Upsilon(nS)\pi$ and $h_b(mP)\pi$ can only happen via $B\bar{B}^* + B^*\bar{B}$ (for simplicity, $B\bar{B}^*$ will be used to represent $B\bar{B}^* + B^*\bar{B}$ in the following) and $B^*\bar{B}^*$ loops. Since both Z_b's are located very close to the corresponding open-bottom threshold, the system can in principle be examined by the NREFT approach.

As shown in Refs. [15,16], a systematic power counting can be established for the π or η emissions between charmonium states. Because the S-wave and P-wave heavy quarkonia couple to the open-flavor heavy meson and antimeson in a P wave and an S wave, respectively, the transitions studied in Ref. [16] can be classified into three groups, namely transitions between the S-wave heavy

*m.cleven@fz-juelich.de
†q.wang@fz-juelich.de
‡fkguo@hiskp.uni-bonn.de
§c.hanhart@fz-juelich.de
‖meissner@hiskp.uni-bonn.de
¶zhaoq@ihep.ac.cn

quarkonium states, P-wave states, and between the P- and S-wave states. The decay amplitudes of different groups have their own nonrelativistic velocity counting. Because the Z_b states have positive parity, they couple to the bottom and antibottom mesons in an S wave. Thus, the transitions $Z_b \to \Upsilon(nS)\pi$ are analogous to those between P- and S-wave quarkonia, while the $Z_b \to h_b(mP)\pi$ processes are similar to those between two P-wave quarkonia. The main difference is that the normal heavy quarkonium transitions with the emission of a pion studied in Ref. [16] break isospin symmetry while the Z_b decays do not. Thus, by studying the $Z_b(Z_b') \to \Upsilon(nS)\pi$ and $h_b(mP)\pi$, we can examine the power counting rules established in Ref. [16], and also better understand the properties of these two exotic states.

Further insight can be gained by studying radiative decays of the neutral Z_b states into bottomonia. Because the $\chi_{bJ}(J = 0, 1, 2)$ states are the spin partners of the h_b of the same principal quantum number, they couple to the bottom mesons with the same coupling constant in the heavy quark limit. Thus, since molecular states can decay via bottom-meson loops only, the radiative decays $Z_b^{(\prime)0} \to \chi_{bJ}(nP)\gamma$ are related to the pionic decays $Z_b^{(\prime)\pm} \to h_b(nP)\pi^{\pm}$. Note that these transitions would be unrelated if the Z_b states were of a tetraquark nature. Similar considerations were made in Ref. [19] for hindered M1 transitions of the P-wave charmonia. These decay channels have not been observed so far, but they could be potentially important in confirming the molecular nature of the Z_b states, and thus are worthwhile to study experimentally.

In this paper, we will assume that the $Z_b^{(\prime)}$ are dynamically generated from the $B^{(*)}\bar{B}^*$ interactions, i.e., hadronic molecules of the $B^{(*)}\bar{B}^*$. We will try to identify the quantities which are sensitive to such a scenario. Section II contributes to the power counting in the NREFT framework of the relevant decays, which are the decays of the Z_b states into the $\Upsilon\pi$, $h_b\pi$, $\chi_{bJ}\gamma$—in particular we show that not all decays are accessible to the formalism. The numerical results are given in Sec. III. In Sec. IV, we compare our results to previous calculations and make some comments. A brief summary is presented in Sec. V. The loop function used in the calculations and the decay amplitudes in the NREFT are collected in Appendix A. As a cross-check, we also calculate the same quantities using a Lorentz covariant formalism, and the formulas are summarized in Appendix B.

II. POWER COUNTING

In Ref. [15], a NREFT method was introduced to study the meson loop effects in the heavy quarkonium transitions. The power counting scheme was analyzed in detail in Ref. [16]. The key quantities here are the velocities of the intermediate mesons. In this section, we briefly review the ideas of Refs. [15,16] together with an improved discussion for the higher loop diagrams.

In general, the heavy meson velocities relevant for the decay of some particle X may be estimated as $v_X \sim \sqrt{|M_X - 2m_B|/m_B}$, where the absolute value indicates that the formula can be used for both bound systems as well as resonances. The analogous formula holds when the two heavy mesons merge to a quarkonium in the final state. According to the rules of a nonrelativistic effective field theory [20] (for a review, see e.g., Ref. [21]), the momentum and nonrelativistic energy count as v_X and v_X^2, respectively. For the integral measure one finds $v_X^5/(4\pi)^2$. The heavy meson propagator counts as $1/v_X^2$. The leading order S-wave vertices do not have any velocity dependence, while the case for the P-wave vertices is more complicated: it scales either as v_X when the momentum due to P-wave coupling contracts with another internal momentum, or as the external momentum q when q is contracted.

We start with the radiative transitions as shown in the upper row of Fig. 1. If the Z_b states are molecular states, their spin wave functions contain both $s_{b\bar{b}} = 0$ and 1 components [4], where $s_{b\bar{b}}$ is the total spin of the $b\bar{b}$ component. Thus, the radiative decays of the Z_b states into the spin-triplet χ_{bJ} can occur without heavy quark spin flip and survive in the heavy quark limit. This is different from the M1 transitions between two P-wave heavy quarkonia which have been analyzed in Ref. [19]. Both the couplings of Z_b and χ_{bJ} to a pair of heavy mesons are in an S wave, and the photon coupling to the bottom

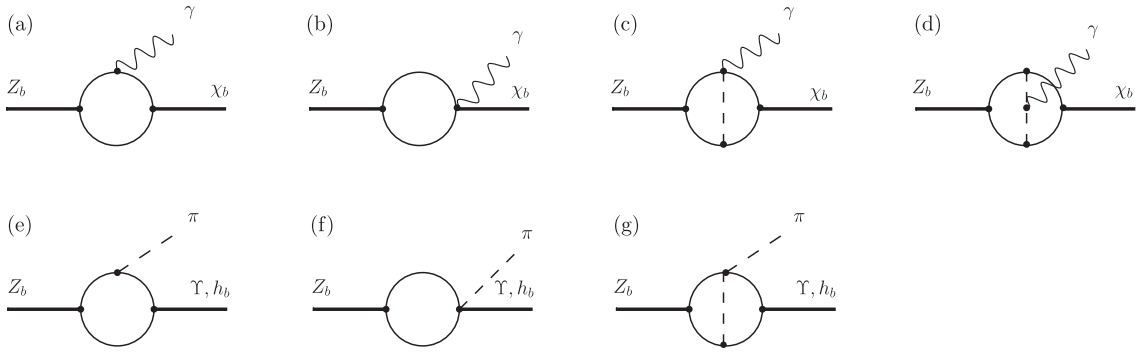

FIG. 1. Schematic one- and two-loop diagrams of the transitions $Z_b \to \Upsilon\pi$, $h_b\pi$ and $\chi_{bJ}\gamma$.

mesons is proportional to the photon energy E_γ. For the diagram of Fig. 1(a) the amplitude therefore scales as

$$\frac{\bar{v}^5}{(4\pi)^2}\frac{1}{(\bar{v}^2)^3}E_\gamma \sim \frac{E_\gamma}{(4\pi)^2\bar{v}}, \tag{1}$$

where the velocity that appears is $\bar{v} = (v_Z + v_\chi)/2 \simeq v_\chi/2$ [22], since $v_Z \sim v_{Z'} \simeq 0.02$, if the central values of the measured $Z_b^{(\prime)}$ masses, 10607.2 MeV and 10652.2 MeV, are used, while v_χ ranges from 0.12 for the $\chi_{bJ}(3P)$ to 0.26 for the $\chi_{bJ}(2P)$ to 0.37 for the $\chi_{bJ}(1P)$. Here we used the mass of the $\chi_{bJ}(3P)$, 10.53 GeV, as reported by the ATLAS Collaboration [23]. In the following, we will count $\bar{v}$ as $\mathcal{O}(v_\chi)$. The scaling ensures that the amplitude gets larger when the bottomonium in the final state is closer to the open-bottom threshold. Thus, we expect for the absolute value of the decay amplitude from this diagram

$$\left|\frac{\mathcal{A}_{\chi_{bJ}(1P)\gamma}}{E_\gamma}\right| : \left|\frac{\mathcal{A}_{\chi_{bJ}(2P)\gamma}}{E_\gamma}\right| : \left|\frac{\mathcal{A}_{\chi_{bJ}(3P)\gamma}}{E_\gamma}\right| \sim \frac{1}{v_{1P}} : \frac{1}{v_{2P}} : \frac{1}{v_{3P}} = 1{:}1.4{:}3.1, \tag{2}$$

if the $\chi_{bJ}(nP)B\bar{B}$ coupling constants take the same value. Diagram (a) can be controlled easily in theory. Thus, clear predictions can be made whenever diagram (a) dominates. In the following we will identify such dominant decays based on the power counting for the NREFT.

As for Fig. 1(b), the coupling $\chi_b B\bar{B}\gamma$ cannot be deduced by gauging the coupling of χ_{bJ} to a $B\bar{B}$-meson pair. Thus, it has to be gauge invariant by itself and proportional to the electromagnetic field strength tensor $F^{\mu\nu}$. This gives a factor of photon energy E_γ and the amplitude of Fig. 1(b) scales as

$$\frac{v_Z^5}{(4\pi)^2}\frac{1}{(v_Z^2)^2}E_\gamma \sim \frac{E_\gamma v_Z}{(4\pi)^2}, \tag{3}$$

where we have assumed that the corresponding coupling is of natural size. Thus, diagram (b) is suppressed compared to diagram (a) at least by a factor of $v_Z v_\chi < 0.01$ for the decay to $\chi_{bJ}(1P)$ and even smaller for the excited states.

The situation is more complicated for the graph displayed in Fig. 1(c). Here we have a two-loop diagram, so that the velocities running in different loops are significantly different—the one in the loop connected to the Z_b is v_Z, and the other is v_χ. It is important to count them separately since $v_Z \ll v_\chi$ due to the very close proximity of the Z_b to the threshold.[1] The internal pion momentum scales as the larger loop momentum, and thus the pion propagator should be $\sim 1/(m_B^2 v_\chi^2)$. This leaves us with

$$\frac{v_Z^5}{(4\pi)^2}\frac{1}{(v_Z^2)^2}\frac{v_\chi^5}{(4\pi)^2}\frac{1}{(v_\chi^2)^2}\frac{1}{m_B^2 v_\chi^2}\frac{E_\gamma g}{F_\pi}\frac{g}{F_\pi}m_B^4 \sim \frac{v_Z}{v_\chi}\frac{E_\gamma g^2 m_B^2}{(4\pi)^2\Lambda_\chi^2}, \tag{4}$$

where F_π is the pion decay constant in the chiral limit, the factor m_B^4 has been introduced to give the same dimension as the estimate for the first two diagrams, and the hadronic scale was introduced via the identification $\Lambda_\chi = 4\pi F_\pi$. Thus the two-loop diagram is suppressed compared to the leading one, Eq. (3), by a factor $v_Z g^2 m_B^2/\Lambda_\chi^2 \sim 0.1$, where we used for the coupling $B^* \to B\pi$ the value $g = 0.5$ (a recent lattice calculation gives 0.449 ± 0.051 [25]), and $\Lambda_\chi \sim 1$ GeV. It can easily be seen that Fig. 1(d) gives the same contribution which also reflects the fact that they are both required at the same order to ensure gauge invariance. Thus, from our power counting it follows that the loop diagrams of Figs. 1(b)–1(d) provide a correction of at most 10%. We will therefore only calculate diagram (a) explicitly and introduce a 10% uncertainty for the amplitudes which corresponds to 20% for the branching ratios. Higher loop contributions are to be discussed later.

Next we consider the hadronic transition $Z_b \to h_b\pi$. This decay has already been studied in Ref. [5] in the same formalism. Again, since the h_b has even parity, its coupling to the bottom mesons is in an S wave. In addition, the final state must be in a P wave to conserve parity, such that the amplitude must be linear in the momentum of the outgoing pion, q. We therefore find for the one-loop contribution of Fig. 1(e)

$$\frac{\bar{v}^5}{(4\pi)^2}\frac{1}{(\bar{v}^2)^3}\frac{gq}{F_\pi} \sim g\frac{qF_\pi}{\bar{v}\Lambda_\chi^2}, \tag{5}$$

while Fig. 1(f) gives

$$\frac{v_Z^5}{(4\pi)^2}\frac{1}{(v_Z^2)^2}\frac{q}{F_\pi} \sim \frac{v_Z q F_\pi}{\Lambda_\chi^2}. \tag{6}$$

Notice that the pion has to be emitted after the loop if the Z_b is a pure hadronic molecule, so that the velocity in the counting should be v_Z instead of v_h. This is suppressed by $v_h v_Z/g$ which leads to a correction of the order of 2% noticing that $v_h \simeq v_\chi$.

The two-loop diagram Fig. 1(g) contributes as

$$\frac{v_Z^5}{(4\pi)^2}\frac{1}{(v_Z^2)^2}\frac{v_\chi^5}{(4\pi)^2}\frac{1}{(v_\chi^2)^2}\frac{1}{m_B^2 v_\chi^2}\frac{gq}{F_\pi}\frac{E_\pi}{F_\pi^2}m_B^3 = \frac{v_Z}{v_h}\frac{gF_\pi q^2 m_B}{\Lambda_\chi^4}, \tag{7}$$

where we have used that the energy from the $\pi B \to \pi B$ vertex can be identified with the energy of the outgoing pion [26], $E_\pi \sim q$. The $B^*B\pi$ vertex contributes a factor of the external momentum q since the $Z_b \to h_b\pi$ is a P-wave decay, and this is the only P-wave vertex. Therefore, this

[1] The concept applied here is analogous to the scheme by now well established for the effective field theory for reactions of the type $NN \to NN\pi$; see Ref. [24] for a review.

diagram is suppressed compared to the leading loop, Eq. (5), by a factor $v_Z m_B q/\Lambda_\chi^2$ which is smaller than 10%. Thus, also for the transitions $Z_b^{(\prime)} h_b \pi$ we may only calculate the leading one-loop diagrams, Fig. 1(e), and assign an uncertainty of 10% to the rates which gives an uncertainty of 20% for the branching ratios. Higher loop contributions are to be discussed later.

Finally, we consider at the decay channel $Z_b \to \Upsilon\pi$. Here the final state is in an S wave, but the coupling of the Υ to $\bar{B}B$ is in a P wave. For diagram (e) the momentum due to this coupling has to scale as the external pion momentum. Together with the pionic coupling that is also linear in the pion momentum, the amplitude is thus proportional to q^2. The one-loop diagram for $Z_b \to \Upsilon\pi$ via Fig. 1(e) is therefore estimated as

$$\frac{\bar{v}^5}{(4\pi)^2}\frac{q}{(\bar{v}^2)^3}\frac{gq}{F_\pi} \sim g\frac{q^2 F_\pi}{\bar{v}\Lambda_\chi^2}. \tag{8}$$

The diagram Fig. 1(f) on the other hand gives

$$\frac{v_Z^5}{(4\pi)^2}\frac{1}{(v_Z^2)^2}\frac{E_\pi}{F_\pi} m_B \sim \frac{v_Z E_\pi F_\pi m_B}{\Lambda_\chi^2}, \tag{9}$$

where m_B is introduced in order to get the same dimension as Eq. (8). Compared to the one-loop diagram (e) this is a relative suppression of order $v_\Upsilon v_Z m_B/q$ which is less than 10% for all the Υ states, where the values of v_Υ are about 0.46, 0.33 and 0.22 for the $1S$, $2S$ and $3S$ states, respectively. The two-loop contribution with the exchange of a pion, Fig. 1(g), is estimated as

$$\frac{v_Z^5}{(4\pi)^2}\frac{1}{(v_Z^2)^2}\frac{v_\Upsilon^5}{(4\pi)^2}\frac{1}{(v_\Upsilon^2)^2}\frac{1}{m_B^2 v_\Upsilon^2}\frac{v_\Upsilon^2 g}{F_\pi}\frac{E_\pi}{F_\pi^2} m_B^5 \sim \frac{v_Z v_\Upsilon g E_\pi F_\pi}{\Lambda_\chi^4} m_B^3. \tag{10}$$

Thus, the strength of the two-loop diagram relative to the leading one-loop diagram is estimated for the $\Upsilon\pi$ as $v_Z v_\Upsilon^2 m_B^3/(\Lambda_\chi^2 q)$. Numerically, this corresponds to a factor of around 0.6 for the $\Upsilon(1S, 2S)\pi$ and 0.7 for the $\Upsilon(3S)\pi$ amplitudes. As a consequence, the branching ratios for these transitions can only be calculated with rather large uncertainties up to 100%.

The heavy meson dimensionless velocities relevant for the mentioned transitions range from 0.02 to 0.5—in momenta this is a range from 0.1 to 2.5 GeV. While pion contributions are expected to be suppressed significantly and can be controlled within chiral perturbation theory for pion momenta of up to 500 MeV and smaller, higher pion loop contributions might get significant for momenta beyond 1 GeV. We will now study those higher pion loops within the power counting scheme outlined above. We will start with the three-loop diagrams, as shown in Fig. 2, considering first diagram (a). The results can be easily generalized to higher loops as shown below. Compared to the two-loop diagrams in Fig. 1, there are one more pion

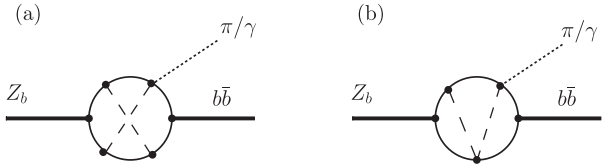

FIG. 2. Two three-loop diagrams contributing to the decays of the Z_b into a heavy quarkonium and a pion or photon.

propagator and two more bottom-meson propagators in the transition and none of them is connected to the external heavy quarkonia. In addition, there is no two-bottom-meson unitary cut present. As a consequence, we have to use a relativistic power counting—cf. Ref. [20]. Then pion momentum and energy are of order $m_B v_{b\bar{b}}$, with $v_{b\bar{b}}$ the velocity of the B meson connected to the $b\bar{b}$ meson in the final state. Both the energies and momenta of the additional bottom mesons are now of the same order, such that the bottom-meson propagator is counted as $1/v_{b\bar{b}}$. The integral measure reads $v_{b\bar{b}}^4/(4\pi)^2$. Therefore, the additional factor as compared to the two-loop diagrams is

$$\frac{v_{b\bar{b}}^4}{(4\pi)^2}\frac{1}{v_{b\bar{b}}^4}\frac{(g v_{b\bar{b}})^2}{F_\pi^2} m_B^2 = \left(\frac{g m_B v_{b\bar{b}}}{\Lambda_\chi}\right)^2. \tag{11}$$

If $v_{b\bar{b}} \sim 0.4$, then the three-loop diagram (a) is of similar size as those of the two-loop diagrams. This is the case for the processes with the $h_b(1P)$, $\chi_{bJ}(1P)$, and $\Upsilon(1S, 2S)$. For smaller values of $v_{b\bar{b}}$, it is suppressed. In diagram (b) there is only one more bottom-meson propagator and the additional $B\pi B\pi$ vertex is in an S wave. We obtain

$$\frac{v_{b\bar{b}}^4}{(4\pi)^2}\frac{1}{v_{b\bar{b}}^3}\frac{v_{b\bar{b}}}{F_\pi^2} m_B^2 = \left(\frac{m_B v_{b\bar{b}}}{\Lambda_\chi}\right)^2. \tag{12}$$

Four and higher loop diagrams that cannot be absorbed by using physical parameters may now be estimated by applying a proper number of factors of the kind of Eqs. (11) and (12). It is easy to see that additional topologies also provide analogous factors. Since $m_B/\Lambda_\chi \sim 5$, higher loops get increasingly important, if $v_{b\bar{b}} > 0.2$. For $v_{b\bar{b}} \sim 0.2$, the three and higher loops are of the same order as the two-loop diagrams, which is the case for the $2P$ states, and thus suppressed in comparison with the one-loop contribution. For the $3P$ bottomonia in the final state, the value of $v_{b\bar{b}}$ is even smaller, and the multiple loops are even suppressed as compared to the two-loop contribution.

To summarize the findings of the power counting analysis, we conclude that the calculation of one-loop triangle diagrams as depicted in Figs. 1(a) and 1(e) is a good approximation, with a controlled uncertainty, to the transitions of the $Z_b^{(\prime)}$ into the $\chi_{bJ}(2P, 3P)\gamma$ and $h_b(2P)\pi$; for the $h_b(3P)\pi$ the phase space is too limited. But similar calculations are not applicable to the decays into the $1P$ states as well as the $\Upsilon(nS)\pi$. For the decays $Z_b \to \Upsilon(nS)\pi$, the contribution from the two-loop diagrams is

TABLE I. Top: Preliminary measurements of the branching ratios for $Z_b^{(\prime)}$ from the Belle Collaboration [2]. Bottom: Masses of the various particles used here [27,28].

Branching ratio (%)	$Z_b(10610)$	$Z_b'(10650)$
$\Upsilon(1S)\pi^+$	0.32 ± 0.09	0.24 ± 0.07
$\Upsilon(2S)\pi^+$	4.38 ± 1.21	2.40 ± 0.63
$\Upsilon(3S)\pi^+$	2.15 ± 0.56	1.64 ± 0.40
$h_b(1P)\pi^+$	2.81 ± 1.10	7.43 ± 2.70
$h_b(2P)\pi^+$	4.34 ± 2.07	14.82 ± 6.22
$B^+\bar{B}^{*0} + \bar{B}^0 B^{*+}$	86.0 ± 3.6	...
$B^{*+}\bar{B}^{*0}$	...	73.4 ± 7.0

	Mass (GeV)		Mass (GeV)
$\Upsilon(1S)$	9.460	$\chi_{b0}(1P)$	9.859
$\Upsilon(2S)$	10.023	$\chi_{b1}(1P)$	9.893
$\Upsilon(3S)$	10.355	$\chi_{b2}(1P)$	9.912
$h_b(1P)$	9.899	$\chi_{b0}(2P)$	10.233
$h_b(2P)$	10.260	$\chi_{b1}(2P)$	10.255
B	5.279	$\chi_{b2}(2P)$	10.269
B^*	5.325	π	0.138

not suppressed or even enhanced compared to the one-loop contribution. In light of this discussion, it becomes clear why the pattern of branching fractions for these channels (see Table I) $\mathcal{B}[\Upsilon(2S)\pi] > \mathcal{B}[\Upsilon(3S)\pi] \gg \mathcal{B}[\Upsilon(1S)\pi]$ cannot be reproduced by calculating the three-point diagrams in the NREFT formalism, which always favors the $1S$ to the $2S$ transition and the $2S$ compared to the $3S$ transition due to the factor q^2 in Eq. (8).

III. RESULTS

In this section, we investigate quantitatively the decays of the Z_b states through heavy meson loops. The coupling of these states to the heavy meson fields $H_a = \vec{V}_a \cdot \sigma + P_a$ and $\bar{H}_a = -\vec{\bar{V}}_a \cdot \vec{\sigma} + \bar{P}_a$ with V_a ($\bar{V}_a$) and P_a ($\bar{P}_a$) annihilating the vector and pseudoscalar (anti)heavy mesons, respectively, is given by the Lagrangian

$$\mathcal{L}_Z = i\frac{z}{2}\langle Z_{ba}^{\dagger i} H_a \sigma^i \bar{H}_b\rangle + \text{H.c.},$$

where the Z_b states are given by a 2×2 matrix

$$Z_{ba}^i = \begin{pmatrix} \frac{1}{\sqrt{2}} Z^{0i} & Z^{+i} \\ Z^{-i} & -\frac{1}{\sqrt{2}} Z^{0i} \end{pmatrix}_{ba}.$$

We incorporate the experimental observation that the $Z_b^{(\prime)}$ couples only to $B^{(*)}\bar{B}^*$ via the Lagrangian,

$$\mathcal{L}_{Z,Z'} = z'\varepsilon^{ijk}\bar{V}^{\dagger i} Z^j V^{\dagger k} + z[\bar{V}^{\dagger i} Z^i P^\dagger - \bar{P}^\dagger Z^i V^{\dagger i}] + \text{H.c.}$$

Fitting to the experimental data we find

$$z = (0.79 \pm 0.05)\,\text{GeV}^{-1/2}, \quad z' = (0.62 \pm 0.07)\,\text{GeV}^{-1/2}, \tag{13}$$

and especially

$$\frac{z}{z'} = 1.27 \pm 0.16 \tag{14}$$

which deviates from unity by 2σ. This deviation indicates a significant amount of spin symmetry violation, which, however, is not unnatural for very-near-threshold states where small differences in masses may imply huge differences in binding energies, resulting in significantly different effective couplings, as already discussed in Ref. [5]. The nonrelativistic Lagrangian for the χ_{bJ} coupling to a pair of heavy mesons can be found in Ref. [29], and the one for the magnetic coupling of heavy mesons in Ref. [30].

With the amplitudes given in Appendix A, it is straightforward to calculate the decay widths of the $Z_b^{(\prime)} \to h_b(mP)\pi$, which are proportional to g_1^2, where g_1 is the P-wave bottomonium—bottom meson coupling constant. In the ratio defined as

$$\xi_m := \frac{\Gamma[Z_b' \to h_b(mP)\pi]}{\Gamma[Z_b \to h_b(mP)\pi]}, \tag{15}$$

g_1 is canceled out. With the meson masses listed in Table I, we obtain

$$\begin{aligned} \xi_1 &= 1.21 \left|\frac{z'}{z}\right|^2 = 0.75, \\ \xi_2 &= (1.53 \pm 0.43) \left|\frac{z'}{z}\right|^2 = 0.95 \pm 0.36, \end{aligned} \tag{16}$$

where the first error in the second term is the theoretical uncertainty due to neglecting higher order contributions (see the discussion in the previous section), and the second one also includes the uncertainty of z'/z added in quadrature. Due to the theoretically uncontrollable higher order contributions for the decays into the $1P$ states, no uncertainty is given for ξ_1.

The predictions are consistent with their experimental counterparts (see Table I)

$$\xi_1^{\text{Exp}} = 1.65 \pm 0.96, \qquad \xi_2^{\text{Exp}} = 2.13 \pm 1.44. \tag{17}$$

Here, new measurements with significantly reduced uncertainties would be very desirable. A collection of ratios for the decays of the Z_b states to $h_b(mP)\pi$ and $\Upsilon(nS)\pi$, respectively, is presented in Table II. The uncertainties, whenever they are under control theoretically, are also included. The significant deviations for the $\Upsilon(nS)\pi$ results from the experimental numbers appear natural, given that for those transitions higher loops were argued to be at least as important as the one-loop diagram included here, as outlined in detail in the previous section. As a cross-check of our nonrelativistic treatment, we also calculated the same quantities using a Lorentz covariant formalism with relativistic propagators for all the intermediate mesons (the formalism is summarized in Appendix B). The results are denoted as "Rel." in Table II. They should be compared

TABLE II. The ratios ξ of different decay modes in both NREFT and a relativistic framework as compared with the experimental data. The NREFT values quoted without uncertainties may be understood as order-of-magnitude estimates.

ξ	NREFT	Rel.	Experiment
$\Upsilon(1S)\pi$	0.7	0.7	0.47 ± 0.22
$\Upsilon(2S)\pi$	0.9	0.8	0.34 ± 0.15
$\Upsilon(3S)\pi$	2 ± 2	1.6	0.48 ± 0.20
$h_b(1P)\pi$	0.8	0.7	1.65 ± 0.96
$h_b(2P)\pi$	1.0 ± 0.4	0.9	2.13 ± 1.44

with the central values of the NREFT results. The difference reflects relativistic corrections to the nonrelativistic treatment of the bottom-meson propagators. In our case, the difference between relativistic and NREFT calculations here and in the following never exceeds 15% for the rates and thus is well below the uncertainty due to higher loops.

It is important to ask to what extent the above predictions can be used to probe the nature of the Z_b states. The Z_b and Z_b' are away from the $B\bar{B}^*$ and $B^*\bar{B}^*$ thresholds by similar distances, $m_{Z_b} - m_B - m_{B^*} \simeq m_{Z_b'} - 2m_{B^*}$. Additionally, due to the heavy quark spin symmetry, one may expect that the loops contribute similarly to the decays of these two states into the same final state. This is indeed the case. We find the ratios after putting $|z'/z|^2$ aside are basically the phase space ratios, which are

$$\frac{|\vec{q}(Z_b' \to h_b(1P)\pi)|^3}{|\vec{q}(Z_b \to h_b(1P)\pi)|^3} = 1.20, \quad \frac{|\vec{q}(Z_b' \to h_b(2P)\pi)|^3}{|\vec{q}(Z_b \to h_b(2P)\pi)|^3} = 1.53. \tag{18}$$

This implies that the ratios for the decays into the $h_b(mP)\pi$ are determined by the ratio of the partial decay widths for the open-bottom decay modes,

$$\xi_m \simeq \frac{\mathrm{PS}_m'}{\mathrm{PS}_m} \frac{\Gamma(Z_b'^+ \to B^{*+}\bar{B}^{*0})}{\Gamma(Z_b^+ \to B^+\bar{B}^0 + B^0\bar{B}^{*+})}, \tag{19}$$

where $\mathrm{PS}_m^{(\prime)}$ is the phase space for the decays $Z_b^{(\prime)} \to h_b(mP)\pi$. Such a relation cannot be obtained if the Z_b states would be of tetraquark structure because the decay of a $\bar{b}\,\bar{q}\,bq$ tetraquark into the $h_b\pi$ knows nothing about the decay into the open-bottom channels. Here, if we impose spin symmetry for z and z', one would get for ξ_m simply the ratio of phase spaces. In reality the second factor which is the square of the ratio of effective couplings, cf. Eq. (14), deviates from unity due to spin symmetry violations enhanced by the proximity of the $B^{(*)}\bar{B}^*$ thresholds as discussed above.

Heavy quark spin symmetry allows one to gain more insight into the molecular structure. Because the $\chi_{bJ}(mP)$ are the spin-multiplet partners of the $h_b(mP)$, the radiative decays of the neutral $Z_b^{(\prime)0}$ into $\chi_{bJ}(mP)\gamma$ can be related to the hadronic decays of the $Z_b^{(\prime)}$, no matter whether they are neutral or charged, into the $h_b(mP)\pi$. It is therefore useful to define the following ratios:

$$\Omega_{[Z_b^{(\prime)},\chi_{bJ}(mP)]} := \frac{\Gamma(Z_b^{(\prime)0} \to \chi_{bJ}(mP)\gamma)}{\Gamma(Z_b^{(\prime)0} \to h_b(mP)\pi^0)}. \tag{20}$$

With the coupling constants in the bottom meson—photon Lagrangian determined from elsewhere (see for instance Ref. [30]), such ratios can be predicted with no free parameters. At the hadronic level, the Z_b radiative transitions can only be related to the hadronic ones if the Z_b's are hadronic molecules so that the two different types of transitions involve the same set of coupling constants (modulo the bottom meson—pion/photon coupling which can be determined from other processes or lattice simulations). Thus, if the branching fractions of the radiative transitions are large enough to be detected, such a measurement would provide valuable information on the nature of the Z_b states. The results for the ratios Ω are collected in Table III.

Using the branching ratio $\mathcal{B}(Z_b^{(\prime)} \to h_b(1P, 2P)\pi^+)$, we find that the branching ratios of $Z_b^{(\prime)} \to \chi_{bJ}(1P, 2P)\gamma$ are of order 10^{-4}–10^{-3}. The largest branching fractions of the $\chi_{bJ}(mP)$ are those into the $\gamma\Upsilon(nS)$, and the $\Upsilon(nS)$ can be easily measured. Thus, the final states for measuring the

TABLE III. The ratio Ω and the corresponding branching fractions for all possible radiative decays. Uncertainties are given whenever they can be controlled theoretically (see text). The values quoted without uncertainties may be understood as order of magnitude estimates.

	Z_b		Z_b'	
	Ω	Branching fraction	Ω	Branching fraction
$\chi_{b0}(1P)\gamma$	5×10^{-3}	1×10^{-4}	4×10^{-3}	3×10^{-4}
$\chi_{b1}(1P)\gamma$	1×10^{-2}	3×10^{-4}	1×10^{-2}	8×10^{-4}
$\chi_{b2}(1P)\gamma$	2×10^{-2}	5×10^{-4}	2×10^{-2}	1×10^{-3}
$\chi_{b0}(2P)\gamma$	$(6.3 \pm 1.8) \times 10^{-3}$	$(2.7 \pm 1.5) \times 10^{-4}$	$(4.2 \pm 1.2) \times 10^{-3}$	$(6.2 \pm 3.2) \times 10^{-4}$
$\chi_{b1}(2P)\gamma$	$(1.3 \pm 0.4) \times 10^{-2}$	$(5.6 \pm 3.2) \times 10^{-4}$	$(1.3 \pm 0.4) \times 10^{-2}$	$(1.9 \pm 1.0) \times 10^{-3}$
$\chi_{b2}(2P)\gamma$	$(1.9 \pm 0.5) \times 10^{-2}$	$(8.3 \pm 4.5) \times 10^{-4}$	$(1.8 \pm 0.5) \times 10^{-2}$	$(2.7 \pm 1.3) \times 10^{-3}$

$Z_b^0 \to \chi_{bJ}\gamma$ would be the same as those of the $Z_b^0 \to \Upsilon(nS)\pi^0$ because the π^0 events are selected from photon pairs. This means that the detection efficiency and background of these two processes would be similar. In the preliminary experimental results [3], the $Z_b(10610)^0$ event number collected in the $\Upsilon(1S, 2S)\pi^0$ channels is of order $\mathcal{O}(100)$. Given that the luminosity of the future Super-KEKB could be 2 orders of magnitude higher than KEKB, such transitions will hopefully be measured. Furthermore, one may also expect to measure these radiative transitions at the LHCb. Note that the experimental confirmation of the ratios given in Table III would be highly nontrivial evidence for the molecular nature of the Z_b states.

Lacking knowledge of the $\chi_{bJ}(3P)B\bar{B}$ coupling constant, the transitions into the $3P$ states cannot be predicted parameter free. However, they can be used to check the pattern in Eq. (2) predicted by the power counting analysis. The decay widths of the $Z_b \to \chi_{bJ}(mP)\gamma$ are proportional to $g^2_{\bar{1},mP}$. Taking the same value for $g^2_{\bar{1},mP}$, the explicit evaluation of the triangle loops gives 1:1.8:4.4 for the ratios defined in Eq. (2) with $J = 1$. The values are close to the ones in Eq. (2), and thus confirm the $1/\bar{v}$ scaling in Eq. (1) of the amplitudes.

As observed in Ref. [16], the NREFT leading loop calculation preserves the heavy quark spin structure. Because the Z_b contains both $s_{b\bar{b}} = 0$ and 1 components, the leading contribution to its transitions into the normal bottomonia, which are eigenstates of $s_{b\bar{b}}$, complies with the spin symmetry. This conclusion should be true no matter what nature the Z_b's have, as long as the spin structure does not change. Thus, one expects that the branching fraction ratios of the decays of the same Z_b into a spin-multiplet bottomonia plus a pion or photon, such as

$$\mathcal{B}(Z_b^{(\prime)} \to \chi_{b0}(mP)\gamma) : \mathcal{B}(Z_b^{(\prime)} \to \chi_{b1}(mP)\gamma) : \mathcal{B}(Z_b^{(\prime)} \to \chi_{b2}(mP)\gamma), \tag{21}$$

are insensitive to the structure of the Z_b. This statement may be confirmed by observing that our results, as shown in Table IV agree with the ratios 1:2.6:4.1 (for the $1P$ states) and 1:2.5:3.8 (for the $2P$ states) which are obtained solely based on heavy quark spin symmetry in Ref. [31]. One may expect a derivation from the spin symmetry results, which is due to the mass difference between the B and B^* mesons, to be of order $\mathcal{O}(2\Lambda_{\rm QCD}/m_B) \sim 10\%$. The central values given in Table IV deviate from the spin symmetry results by at most 20%, and they are fully consistent considering the uncertainties.

TABLE IV. The ratios defined in Eq. (21) for all channels. Uncertainties are given whenever they can be controlled theoretically.

	$(J = 0):(J = 1):(J = 2)$
$Z_b \to \chi_{bJ}(1P)\gamma$	1:2.5:3.7
$Z_b' \to \chi_{bJ}(1P)\gamma$	1:2.9:4.4
$Z_b \to \chi_{bJ}(2P)\gamma$	$1:(2.1 \pm 0.6):(2.9 \pm 0.8)$
$Z_b' \to \chi_{bJ}(2P)\gamma$	$1:(3.0 \pm 0.9):(4.2 \pm 1.2)$

IV. COMPARISON WITH OTHER WORKS ON Z_b DECAYS

Since their discovery in an impressive number of theoretical works the molecular nature of the Z_b states has been investigated. In this section we compare in some detail our approach to the calculations in Refs. [32–35] which deal with some of the decays considered in our paper. Common to most of these works is that, contrary to our approach, the second part of the one-loop integral shown in Fig. 1(e) is either approximated [32,33] or calculated differently [34]. In particular, the analytic structure of the loop is changed by converting it to a topology of type (f) in Fig. 1, since the second $B^{(*)}\bar{B}^{(*)}$ cut was removed from the loop. However, our power counting gives that it is exactly this cut that drives the enhancement of the one-loop diagrams compared to the two-loop diagrams.

Since the loop of type (f) gives the wave function at the origin in r space, the formalism applied in Refs. [32–34] is basically identical to that used in the classic calculations for the decay of positronium into two photons. However, as discussed in detail in Ref. [36], it is applicable only if the range of the transition potential from the constituents to the final state is significantly shorter than the potential that formed the molecule—a scale not to be mixed up with the size of the molecule which can be very large for a shallow bound state. However, the range of the binding momentum of the Z_b states is not known and might well be of the order of the range of the transition potential (at least as long as the final bottomonium is not a ground state). In such a situation in Ref. [36] it was proposed to calculate the full loop function for the transitions, as done here in our work, which in effect means to expand around the limit of a zero range potential that forms the bound state. In that paper it was also shown that the potentially most important corrections to the transition rate cancel, such that the uncertainty of the procedure is given by the binding momentum of the molecule in units of the range of forces and not of the order of the final momenta in units of the range of forces. This gives an additional justification for the approach we are using. We now discuss the formalisms of Refs. [32–35] in some more detail.

In Ref. [32] an effective field theory called X-EFT was used. It is valid for hadronic molecules with small binding energies so that the pion mass and the heavy meson hyperfine splitting are hard scales. The decays of the $Z_b^{(\prime)}$ can be represented by a bubble with two vertices: one connects the $B^{(*)}\bar{B}^*$ to the $Z_b^{(\prime)}$ states and the other is a local operator for the $B^{(*)}\bar{B}^*\pi(\bar{b}b)$ coupling. The coefficient of the local operator depends on the pion energy, and is obtained by

matching to the tree-level diagrams in heavy hadron chiral perturbation theory. For more details, we refer to Refs. [29,37]. The ratios of $\Gamma(Z' \to \Upsilon(3S)\pi)/\Gamma(Z \to \Upsilon(3S)\pi)$ and $\Gamma(Z' \to h_b(2P)\pi)/\Gamma(Z \to h_b(2P)\pi)$ were calculated in Ref. [32], assuming $z = z'$. As outlined in the discussion below Eq. (19), in this case these ratios are just the ratios of phase spaces and thus our results for them agree for $z = z'$. The method of Ref. [33] is a phenomenological variant of the approach outlined above.

Also in Ref. [34] the transition from the intermediate $B^{(*)}\bar{B}^*$ system to the final $\pi(\bar{b}b)$ system was assumed to be local; however, here the strength of this local operator was calculated differently: the authors estimate it via the overlap integral of the $\bar{b}b$ component in the $B^{(*)}\bar{B}^*$ wave function with the outgoing $\bar{b}b$ pair in the presence of a dipole operator. While this procedure is certainly justified when there are $1P$ states in the final state—here the relative momenta between the two B mesons are beyond 2.5 GeV and indeed in this case our effective field theory does not converge anymore (cf. Sec. II)—we regard it as questionable for the $2P$ states. There is one more difference, namely the fact that in the formalism of Ref. [34], the transitions to the $\gamma\chi_{bJ}(nP)$ final states are disconnected from those to the $\pi h_b(nP)$ states, while in our approach they are connected as discussed in detail above. Thus, an experimental observation of the decay of one of the Z_b states to, say, $\gamma\chi_{bJ}(2P)$ would allow one to decide on the applicability of our approach.

Similar to our work, in Ref. [35] the full heavy meson loop is evaluated, but regularized with a form factor. Absolute predictions are given for the transitions using a model to estimate the $B^{(*)}\bar{B}^{(*)}(\bar{b}b)$ coupling—it is difficult to judge the uncertainty induced by this. In a first step in that work a cutoff parameter was adjusted to reproduce each individual transition. It is found that the cutoff parameters needed for the $h_b\pi$ transitions are typically larger and closer together than those needed for the $\Upsilon\pi$ transitions. This hints at form factor effects being not very significant in the former decays. This interpretation is also supported by the observation that the ratios of decay rates—the same quantities as investigated here—are found to be basically independent of the form factor. In this sense the phenomenological studies of Ref. [35] provide additional support for the effective field theory calculation presented here, although a well-controlled error estimate cannot be expected from such a method.

V. SUMMARY

In this paper, we assume that both Z_b and Z_b' are hadronic molecules predominantly coupling to $B\bar{B}^*$ and $B^*\bar{B}^*$, respectively, in line with the data by the Belle Collaboration. As a consequence of this assumption, the Z_b states can only couple through $B^{(*)}\bar{B}^*$ loops. Using NREFT power counting we argue that

(i) the decay channels $Z_b^{(\prime)} \to \Upsilon(nS)\pi$ as well as the transitions into the ground state P-wave bottomonia in the final state cannot be controlled within the effective field theory, since higher loop contributions are expected to dominate the transitions;

(ii) model-independent predictions can be provided for $Z_b^{(\prime)} \to h_b(2P)\pi$ and radiative decays $Z_b^{(\prime)} \to \chi_{bJ}(2P)\gamma$.

The ratios for Z_b and Z_b' decays into the same final states $h_b(mP)\pi$ are consistent with the experimental data. Our results reflect the fact that those ratios are essentially the ratio of the corresponding phase space factors times the ratio of the $Z_bB\bar{B}^*$ and $Z_b'B^*\bar{B}^*$ couplings squared. If further experimental analysis with higher statistics could underpin this fact, it would be a very strong evidence for the molecular interpretation since such a relation cannot be obtained from, e.g., a tetraquark structure.

Furthermore, we calculate branching fractions for the final states $\chi_{bJ}(mP)\gamma$. They are predicted to be of order 10^{-4}–10^{-3}. Although this is clearly a challenge to experimentalists, a confirmation of these rates would strongly support the molecular picture. It is noted that the ratios of a certain Z_b into bottomonia in the same spin multiplet are insensitive to the structure of the Z_b, and may be obtained solely based on heavy quark spin symmetry.

ACKNOWLEDGMENTS

We would like to thank M. Voloshin for valuable discussions. This work is supported in part by the DFG and the NSFC through funds provided to the Sino-German CRC 110 "Symmetries and the Emergence of Structure in QCD," the EU I3HP "Study of Strongly Interacting Matter" under the Seventh Framework Program of the EU, and the NSFC (Grants No. 11035006, No. 11121092, and No. 11165005).

APPENDIX A: NONRELATIVISTIC APPROACH

The basic three-point loop function worked out using dimensional regularization in $D = 4$ is

$$I(m_1, m_2, m_3, \vec{q}) = \frac{-i}{8}\int \frac{d^D l}{(2\pi)^D} \frac{1}{[l^0 - \frac{\vec{l}^2}{m_1} + i\epsilon]} \frac{1}{[l^0 + b_{12} + \frac{\vec{l}^2}{m_2} - i\epsilon]} \frac{1}{[l^0 + b_{12} - b_{23} - \frac{(\vec{l}-\vec{q})^2}{m_3} + i\epsilon]}$$
$$= \frac{\mu_{12}\mu_{23}}{16\pi}\frac{1}{\sqrt{a}}\left[\tan^{-1}\left(\frac{c' - c}{2\sqrt{a(c - i\epsilon)}}\right) + \tan^{-1}\left(\frac{2a + c - c'}{2\sqrt{a(c' - a - i\epsilon)}}\right)\right], \tag{A1}$$

where $m_i (i = 1, 2, 3)$ are the masses of the particles in the loop; $\mu_{ij} = m_i m_j/(m_i + m_j)$ are the reduced masses; $b_{12} = m_1 + m_2 - M$ and $b_{23} = m_2 + m_3 + q^0 - M$, with M the mass of the initial particle; and

$$a = \left(\frac{\mu_{23}}{m_3}\right)^2 \vec{q}^2, \quad c = 2\mu_{12} b_{12}, \quad c' = 2\mu_{23} b_{23} + \frac{\mu_{23}}{m_3}\vec{q}^2.$$

In terms of the loop function given above, the amplitudes for Z_b^+ and $Z_b'^+$ decays into $h_b \pi^+$ are

$$\mathcal{A}_{Z_b^+ h_b} = \frac{2\sqrt{2} g g_1 z_1}{F_\pi}\sqrt{M_{h_b} M_{Z_b}}\epsilon_{ijk} q^i \varepsilon_{Z_b}^j \varepsilon_{h_b}^k \times [I(M_B, M_{B^*}, M_{B^*}, \vec{q}) + I(M_{B^*}, M_B, M_{B^*}, \vec{q})] \tag{A2}$$

and

$$\mathcal{A}_{Z_b'^+ h_b} = \frac{2\sqrt{2} g g_1 z_2}{F_\pi}\sqrt{M_{h_b} M_{Z_b'}}\epsilon_{ijk} q^i \varepsilon_{Z_b'}^j \varepsilon_{h_b}^k \times [I(M_{B^*}, M_{B^*}, M_B, \vec{q}) + I(M_{B^*}, M_{B^*}, M_{B^*}, \vec{q})], \tag{A3}$$

respectively. In all these amplitudes, both the neutral and charged bottom and antibottom mesons have been taken into account. The amplitudes for $Z_b^{(\prime)0}$ into $\chi_{bJ}\gamma$ read

$$\mathcal{A}_{Z_b^0 \chi_{b0}\gamma} = -\sqrt{\frac{2}{3}} i\beta e g_1 z \sqrt{M_{\chi_b} M_{Z_b}}\epsilon_{ijk} q^i \varepsilon_{Z_b}^j \varepsilon_\gamma^k \times [I(M_B, M_{B^*}, M_{B^*}, \vec{q}) - 3I(M_{B^*}, M_B, M_B, \vec{q})], \tag{A4}$$

$$\mathcal{A}_{Z_b'^0 \chi_{b0}\gamma} = -2i\sqrt{\frac{2}{3}}\beta e g_1 z' \sqrt{M_{\chi_b} M_{Z_b}}\epsilon_{ijk} q^i \varepsilon_{Z_b}^j \varepsilon_\gamma^k \times I(M_{B^*}, M_{B^*}, M_{B^*}, \vec{q}), \tag{A5}$$

$$\mathcal{A}_{Z_b^0 \chi_{b1}\gamma} = 2i\beta e g_1 z \sqrt{M_{\chi_b} M_{Z_b}}(q^i g^{jk} - q^k g^{ij})\varepsilon_{Z_b}^i \varepsilon_\gamma^j \varepsilon_{\chi_b}^k \times I(M_{B^*}, M_B, M_{B^*}, \vec{q}), \tag{A6}$$

$$\mathcal{A}_{Z_b'^0 \chi_{b1}\gamma} = -2i\beta e g_1 z \sqrt{M_{\chi_b} M_{Z_b}}(q^i g^{jk} - q^k g^{ij})\varepsilon_{Z_b}^i \varepsilon_\gamma^j \varepsilon_{\chi_b}^k \times I(M_{B^*}, M_{B^*}, M_B, \vec{q}), \tag{A7}$$

and

$$\mathcal{A}_{Z_b^0 \chi_{b2}\gamma} = \sqrt{2} i\beta e g_1 z \sqrt{M_{\chi_b} M_{Z_b}} q^i (g^{jm}\varepsilon_{ikl} + g^{jl}\varepsilon_{ikm}) \times \varepsilon_{Z_b}^j \varepsilon_\gamma^k \varepsilon_{\chi_b}^{lm} I(M_{B^*}, M_{B^*}, M_{B^*}, \vec{q}), \tag{A8}$$

$$\mathcal{A}_{Z_b'^0 \chi_{b2}\gamma} = \sqrt{2} i\beta e g_1 z \sqrt{M_{\chi_b} M_{Z_b}}(q^i (g^{jm}\varepsilon_{ikl} + g^{jl}\varepsilon_{ikm}) + q^l \varepsilon^{ijm} + q^m \varepsilon^{ijl})\varepsilon_{Z_b}^j \varepsilon_\gamma^k \varepsilon_{\chi_b}^{lm} I(M_{B^*}, M_{B^*}, M_{B^*}, \vec{q}), \tag{A9}$$

respectively.

APPENDIX B: RELATIVISTIC APPROACH

In this appendix, we formulate a Lorentz covariant framework for a parallel study of the $Z_b^{(\prime)}$ decays. In such a framework, more terms will appear as relativistic corrections that are generally neglected in the heavy quark limit. Therefore, a comparison between these two prescriptions will serve as a cross-check of the NREFT results, and more importantly as a confirmation of the validity of the NREFT power counting.

The bottom-meson fields are defined as

$$H_1 = \left(\frac{1+\not{v}}{2}\right)[P_\mu^* \gamma^\mu - \gamma_5 P],$$
$$H_1^\dagger = \gamma^0 [P_\mu^{*\dagger}\gamma^\mu + \gamma_5 P^\dagger]\left(\frac{1+\not{v}}{2}\right)\gamma^0,$$
$$\bar{H}_1 = \gamma^0 H_1^\dagger \gamma^0,$$
$$H_2 = [\bar{P}_\mu^* \gamma^\mu - \gamma_5 \bar{P}]\left(\frac{1-\not{v}}{2}\right),$$
$$H_2^\dagger = \gamma^0\left(\frac{1-\not{v}}{2}\right)[\bar{P}_\mu^{*\dagger}\gamma^\mu + \gamma_5 \bar{P}^\dagger]\gamma^0,$$
$$\bar{H}_2 = \gamma^0 H_2^\dagger \gamma^0,$$

where P^* and P represent the $(B^{*+}, B^{*0}, B_s^{*0})$ and (B^+, B^0, B_s^0) fields, respectively, which annihilate the corresponding particles, while $\bar{P}^*$ and $\bar{P}$ are the fields of their antiparticles. The fields annihilating the S- and P-wave bottomonia are given by

$$R_{b\bar{b}} = \left(\frac{1+\not{v}}{2}\right)(\Upsilon^\mu \gamma_\mu - \eta_b \gamma_5)\left(\frac{1-\not{v}}{2}\right),$$
$$P_{b\bar{b}}^\mu = \left(\frac{1+\not{v}}{2}\right)\Big[\chi_{b2}^{\mu\alpha}\gamma_\alpha + \frac{1}{\sqrt{2}}\epsilon^{\mu\nu\alpha\beta} v_\alpha \gamma_\beta \chi_{b1\nu} + \frac{1}{\sqrt{3}}(\gamma^\mu - v^\mu)\chi_{b0} + h_b^\mu \gamma_5\Big]\left(\frac{1-\not{v}}{2}\right),$$

respectively. The Lagrangians for S-wave (P-wave) quarkonia and a pair of heavy mesons are

$$\mathcal{L}_{SB\bar{B}} = ig_2 \mathrm{Tr}[R_{b\bar{b}} \bar{H}_{2a} \gamma^\mu \overleftrightarrow{\partial}_\mu \bar{H}_{1a}] + \mathrm{H.c.}, \tag{B1}$$

$$\mathcal{L}_{PB\bar{B}} = ig_1 \mathrm{Tr}[P_{b\bar{b}}^\mu \bar{H}_{2a}\gamma_\mu \bar{H}_{1a}] + \mathrm{H.c.} \tag{B2}$$

Under the similar convention, the Z_b field can be expressed as

$$P_Z^\mu = \left(\frac{1+\not{v}}{2}\right)Z^\mu \gamma_5 \left(\frac{1-\not{v}}{2}\right), \tag{B3}$$

and the effective interaction between the Z_b and a pair of bottomed meson reads

$$\mathcal{L}_{ZB\bar{B}} = iz^{(\prime)}\mathrm{Tr}[P_{Z,ab}^{\dagger\mu}\bar{H}_{2b}\gamma_\mu \bar{H}_{1a}] + \mathrm{H.c.} \tag{B4}$$

The Lagrangian for the pion coupling to a pair of bottom mesons is [38–40]

$$\mathcal{L} = ig\mathrm{Tr}[H_b\gamma_\mu\gamma_5\mathcal{A}^\mu_{ba}\bar{H}_a], \tag{B5}$$

where $\mathcal{A}_\mu = (\xi^\dagger\partial_\mu\xi - \xi\partial_\mu\xi^\dagger)/2$, with $\xi = \exp(i\sqrt{2}\phi/F_\pi)$. The relativistic form of the Lagrangian for the photon coupling to the bottom mesons is [30]

$$\mathcal{L}_\gamma = \frac{e\beta Q_{ab}}{2}F^{\mu\nu}\mathrm{Tr}[H_b^\dagger\sigma_{\mu\nu}H_a] + \frac{eQ'}{2m_Q}F^{\mu\nu}\mathrm{Tr}[H_a^\dagger H_a\sigma_{\mu\nu}]. \tag{B6}$$

With these effective Lagrangians, we obtain for the amplitudes of $Z_b^{(\prime)} \to h_b\pi$

$$\mathcal{A}_{Z_b h_b} = \frac{2\sqrt{2}gg_1z}{F_\pi}\epsilon_{qv\epsilon_{h_b}\epsilon_{Z_b}}(C_0[M_B, M_{\bar{B}^*}, M_{B^*}] + C_0[M_{B^*}, M_{\bar{B}}, M_{B^*}]), \tag{B7}$$

$$\mathcal{A}_{Z'_b h_b} = \frac{2\sqrt{2}gg_1z}{F_\pi}\epsilon_{qv\epsilon_{h_b}\epsilon_{Z_b}}(C_0[M_{B^*}, M_{\bar{B}^*}, M_{B^*}] + C_0[M_{B^*}, M_{\bar{B}^*}, M_B]), \tag{B8}$$

and to $\Upsilon\pi$

$$\mathcal{A}_{Z_b\Upsilon} = \frac{2\sqrt{2}gg_2z}{F_\pi}(-\epsilon_\Upsilon\cdot\epsilon_Z|\vec{q}|^2(C_0[M_B, M_{\bar{B}^*}, M_{B^*}] + 2C_2[M_B, M_{\bar{B}^*}, M_{B^*}] + C_0[M_{B^*}, M_{\bar{B}}, M_{B^*}] + 2C_2[M_{B^*}, M_{\bar{B}}, M_{B^*}]) + q\cdot\epsilon_\Upsilon q\cdot\epsilon_Z(C_0[M_{B^*}, M_{\bar{B}}, M_B] + 2C_2[M_{B^*}, M_{\bar{B}}, M_B] - C_0[M_{B^*}, M_{\bar{B}}, M_{B^*}] - 2C_2[M_{B^*}, M_{\bar{B}}, M_{B^*}])), \tag{B9}$$

$$\mathcal{A}_{Z'_b\Upsilon} = \frac{2\sqrt{2}gg_2z}{F_\pi}(\epsilon_Z\cdot\epsilon_\Upsilon|\vec{q}|^2(C_0[M_{B^*}, M_{\bar{B}^*}, M_B] + C_2[M_{B^*}, M_{\bar{B}^*}, M_B] + C_0[M_{B^*}, M_{\bar{B}^*}, M_{B^*}] + C_2[M_{B^*}, M_{\bar{B}^*}, M_{B^*}]) + q\cdot\epsilon_\Upsilon q\cdot\epsilon_Z(C_0[M_{B^*}, M_{\bar{B}^*}, M_B] + C_2[M_{B^*}, M_{\bar{B}^*}, M_B] - C_0[M_{B^*}, M_{\bar{B}^*}, M_{B^*}] - C_2[M_{B^*}, M_{\bar{B}^*}, M_{B^*}])). \tag{B10}$$

The amplitudes for $Z_b^{(\prime)} \to \chi_{b0}\gamma$ are

$$A_{Z_b^0\chi_{b0}\gamma} = i\frac{\beta e g_1 z\sqrt{2}}{\sqrt{3}}\epsilon_{qv\epsilon_\gamma\epsilon_{Z_b}}(3C_0[M_{B^*}, M_{\bar{B}}, M_B] - C_0[M_B, M_{\bar{B}^*}, M_{B^*}]) \tag{B11}$$

$$A_{Z_b^0\chi_{b1}\gamma} = i2eg_1z\beta(\epsilon_{\chi_{b1}}\cdot\epsilon_\gamma q\cdot\epsilon_Z - q\cdot\epsilon_{\chi_{b1}}\epsilon_\gamma\cdot\epsilon_Z)C_0[M_{B^*}, M_{\bar{B}}, M_{B^*}] \tag{B12}$$

$$A_{Z_b^0\chi_{b2}\gamma} = i2\sqrt{2}eg_1z\beta\epsilon_Z^\sigma\epsilon^{\alpha qv\epsilon_\gamma}\epsilon_{\chi_{b2}\sigma\alpha}C_0[M_B, M_{\bar{B}^*}, M_{B^*}], \tag{B13}$$

and

$$A_{Z_b^{\prime 0}\chi_{b0}\gamma} = -2\frac{\sqrt{2}}{\sqrt{3}}ieg_1z'\beta\epsilon_{qv\epsilon_\gamma\epsilon_Z}C_0[M_{B^*}, M_{\bar{B}^*}, M_{B^*}] \tag{B14}$$

$$A_{Z_b^{\prime 0}\chi_{b1}\gamma} = -i2eg_1z'\beta(\epsilon_{\chi_{b1}}\cdot\epsilon_\gamma q\cdot\epsilon_Z - q\cdot\epsilon_{\chi_{b1}}\epsilon_\gamma\cdot\epsilon_Z)C_0[M_{B^*}, M_{\bar{B}^*}, M_{B^*}] \tag{B15}$$

$$A_{Z_b^{\prime 0}\chi_{b2}\gamma} = i2\sqrt{2}eg_1z'\beta(q^\alpha\epsilon_{\sigma v\epsilon_\gamma\epsilon_Z} + \epsilon_\gamma^\alpha\epsilon_{\sigma qv\epsilon_Z})\chi_{b2\alpha}^\sigma C_0[M_{B^*}, M_{\bar{B}^*}, M_{B^*}], \tag{B16}$$

respectively. Here, C_0 is the standard relativistic three-point scalar function which is similar to the definition of I in Appendix A

$$C_0[p^2, (-q)^2, (p-q)^2, m_2^2, m_1^2, m_3^2] = \frac{(2\pi\mu)^{4-D}}{i\pi^2}\int\frac{d^Dl}{(l^2-m_1^2)((p-l)^2-m_2^2)((l-q)^2-m_3^2)}, \tag{B17}$$

where the incoming four-momentum of the Z_b is p, and the light outgoing particle four-momentum is q. For simplicity, we do not explicitly include the first three arguments in C_0 in the above formulas. With the same convention, C_2 is a coefficient that arises from the tensor reduction of the three-point vector loop,

$$C^\mu \equiv \frac{(2\pi\mu)^{4-D}}{i\pi^2}\int\frac{l^\mu d^Dl}{(l^2-m_1^2)((p-l)^2-m_2^2)((l-q)^2-m_3^2)} = C_1p^\mu + C_2(p-q)^\mu, \tag{B18}$$

which is similar to the integral I_1 defined in Ref. [16].

To compare with the NREFT method, we note the following treatments in the heavy quark limit:

(i) By expressing the heavy meson momentum $M_Q v_\mu = m_Q v_\mu + k_\mu$ in the heavy quark limit, where v is the heavy meson velocity and k is the residual momentum of the order of Λ_{QCD}, the derivative in Eq. (B1) only gives the difference of the residual momentum between the intermediate bottomed mesons [41]. Namely, the residual momentum k is the integral momentum in the meson loops instead of v.

(ii) The denominators $(l^2 - m_1^2)((p-l)^2 - m_2^2) \times ((l-q)^2 - m_3^2)$ of the meson loops contain two independent external momenta p and q. For the incoming momentum p, we set $p = M_Z v$ following the convention of Ref. [16], where $v = (1, 0, 0, 0)$ defines the rest frame of the initial particle. By doing this, the vector three-point function defined in the loop integrals becomes $C^\mu = M_Z v^\mu C_1 + (M_Z v^\mu - q^\mu) C_2$ which can be compared with the NREFT amplitudes term by term. It is interesting to note that the coefficient of C_1 vanishes in the decay amplitude because of cancellation.

(iii) Another difference between this scheme and the NREFT comes from the contraction term $q \cdot \epsilon_\Upsilon$, where q is the external light meson (e.g., pion) momentum. Note that the time component appears as an additional contribution compared to the NREFT formalism. It is proportional to $|\vec{q}| E_\pi / m_\Upsilon$, which is a relativistic correction and relatively suppressed with respect to the space component $|\vec{q}| E_\Upsilon / m_\Upsilon$.

(iv) The relativistic corrections also arise from the mass difference between m_B and m_{B^*}. One notices that in Eqs. (B9) and (B10), the terms proportional to $q \cdot \epsilon_\Upsilon q \cdot \epsilon_Z$ are given by the D-wave transition. In the heavy quark limit with $m_B = m_{B^*}$, exact cancellations occur within the integral functions C_0 and C_2, respectively. This means if the Z_b and Z_b' are indeed the $B\bar{B}^*$ and $B^*\bar{B}^*$ molecular states, respectively, their D-wave decays into the $\Upsilon\pi$ will be highly suppressed. This can be understood by noticing that the heavy quark spin decouples from the system in the heavy quark limit, and the total angular momentum of the light quarks $s_{q\bar{q}}$ is a good quantum number. If the $Z_b^{(\prime)}$ states are S-wave $B^{(*)}\bar{B}^*$ hadronic molecules as assumed here, there is no spatial angular momentum in the system. Thus, the light quark system has $s_{q\bar{q}} = 0$ or 1, and therefore cannot couple to a spinless pion in a D wave. A similar statement was made very recently in Ref. [42]. Here we notice that the decay of a $b\bar{b}q\bar{q}$ tetraquark state with $s^P_{q\bar{q}} = 2^-$ would decay into $b\bar{b}\pi$ dominantly in a D wave.

(v) We also note the convention for the sums of the polarizations for the vector and tensor particles: $\epsilon^\mu_{\Upsilon(h_b,\chi_{b_1})} \epsilon^{*\nu}_{\Upsilon(h_b,\chi_{b_1})} = -g^{\mu\nu} + v^\mu v^\nu \equiv \tilde{g}^{\mu\nu}$ and $\epsilon^{\mu\nu}_{\chi_{b2}} \epsilon^{*\alpha\beta}_{\chi_{b2}} = \frac{1}{2}(\tilde{g}^{\mu\alpha}\tilde{g}^{\nu\beta} + \tilde{g}^{\mu\beta}\tilde{g}^{\nu\alpha}) - \frac{1}{3}\tilde{g}^{\mu\nu}\tilde{g}^{\alpha\beta}$. They allow us to separate out the relativistic contributions in the scalar loop diagrams which can then be compared with the NREFT formulas explicitly.

The relativistic formalism is advantageous for providing a cross-check of the NREFT results and singling out the effects arising from the relativistic corrections. For the bottomonium and bottomed meson system discussed here, it shows that the relativistic corrections are indeed small and these two methods are consistent with each other. Alternatively, it should be cautioned that in the relativistic formalism, when the terms proportional to $|\vec{q}| E_\pi / m_{Q\bar{Q}}$ are not obviously suppressed in comparison with the three-momentum $|\vec{q}|$, i.e., $E_\pi / m_{Q\bar{Q}}$ is sizeable, a different scheme with a form factor [43,44] might be used to control the large momentum contributions and nonlocal effects of each coupling.

[1] A. Bondar *et al.* (Belle Collaboration), Phys. Rev. Lett. **108**, 122001 (2012).
[2] I. Adachi *et al.* (Belle Collaboration), arXiv:1209.6450.
[3] I. Adachi *et al.* (Belle Collaboration), arXiv:1207.4345.
[4] A. E. Bondar, A. Garmash, A. I. Milstein, R. Mizuk, and M. B. Voloshin, Phys. Rev. D **84**, 054010 (2011).
[5] M. Cleven, F.-K. Guo, C. Hanhart, and U.-G. Meißner, Eur. Phys. J. A **47**, 120 (2011).
[6] J. Nieves and M. P. Valderrama, Phys. Rev. D **84**, 056015 (2011).
[7] J.-R. Zhang, M. Zhong, and M.-Q. Huang, Phys. Lett. B **704**, 312 (2011).
[8] Y. Yang, J. Ping, C. Deng, and H.-S. Zong, J. Phys. G **39**, 105001 (2012).
[9] Z.-F. Sun, J. He, X. Liu, Z.-G. Luo, and S.-L. Zhu, Phys. Rev. D **84**, 054002 (2011).
[10] S. Ohkoda, Y. Yamaguchi, S. Yasui, K. Sudoh, and A. Hosaka, Phys. Rev. D **86**, 014004 (2012).
[11] M. T. Li, W. L. Wang, Y. B. Dong, and Z. Y. Zhang, J. Phys. G **40**, 015003 (2013).
[12] H.-W. Ke, X.-Q. Li, Y.-L. Shi, G.-L. Wang, and X.-H. Yuan, J. High Energy Phys. 04 (2012) 056.
[13] T. Guo, L. Cao, M.-Z. Zhou, and H. Chen, arXiv:1106.2284.

[14] A. Ali, C. Hambrock, and W. Wang, Phys. Rev. D **85**, 054011 (2012).
[15] F.-K. Guo, C. Hanhart, and U.-G. Meißner, Phys. Rev. Lett. **103**, 082003 (2009); **104**, 109901(E) (2010).
[16] F.-K. Guo, C. Hanhart, G. Li, U.-G. Meißner, and Q. Zhao, Phys. Rev. D **83**, 034013 (2011).
[17] S. Weinberg, Phys. Rev. **137**, B672 (1965).
[18] V. Baru, J. Haidenbauer, C. Hanhart, Y. Kalashnikova, and A. E. Kudryavtsev, Phys. Lett. B **586**, 53 (2004).
[19] F.-K. Guo and U.-G. Meißner, Phys. Rev. Lett. **108**, 112002 (2012).
[20] D. B. Kaplan, arXiv:nucl-th/0510023.
[21] N. Brambilla, A. Pineda, J. Soto, and A. Vairo, Rev. Mod. Phys. **77**, 1423 (2005).
[22] F.-K. Guo and U.-G. Meißner, Phys. Rev. Lett. **109**, 062001 (2012).
[23] G. Aad *et al.* (ATLAS Collaboration), Phys. Rev. Lett. **108**, 152001 (2012).
[24] C. Hanhart, Phys. Rep. **397**, 155 (2004).
[25] W. Detmold, C.-J. D. Lin, and S. Meinel, Phys. Rev. Lett. **108**, 172003 (2012).
[26] V. Lensky, V. Baru, J. Haidenbauer, C. Hanhart, A. E. Kudryavtsev, and U.-G. Meißner, Eur. Phys. J. A **27**, 37 (2006).
[27] I. Adachi *et al.* (Belle Collaboration), Phys. Rev. Lett. **108**, 032001 (2012).
[28] J. Beringer *et al.* (Particle Data Group), Phys. Rev. D **86**, 010001 (2012).
[29] S. Fleming and T. Mehen, Phys. Rev. D **78**, 094019 (2008).
[30] J. Hu and T. Mehen, Phys. Rev. D **73**, 054003 (2006).
[31] S. Ohkoda, Y. Yamaguchi, S. Yasui, and A. Hosaka, Phys. Rev. D **86**, 117502 (2012).
[32] T. Mehen and J. W. Powell, Phys. Rev. D **84**, 114013 (2011).
[33] Y. Dong, A. Faessler, T. Gutsche, and V. E. Lyubovitskij, J. Phys. G **40**, 015002 (2013).
[34] X. Li and M. B. Voloshin, Phys. Rev. D **86**, 077502 (2012).
[35] G. Li, F. L. Shao, C. W. Zhao, and Q. Zhao, arXiv:1212.3784.
[36] C. Hanhart, Yu. Kalashnikova, A. Kudryavtsev, and A. Nefediev, Phys. Rev. D **75**, 074015 (2007).
[37] S. Fleming, M. Kusunoki, T. Mehen, and U. van Kolck, Phys. Rev. D **76**, 034006 (2007).
[38] G. Burdman and J. F. Donoghue, Phys. Lett. B **280**, 287 (1992).
[39] M. B. Wise, Phys. Rev. D **45**, R2188 (1992).
[40] T. M. Yan, H. Y. Cheng, C. Y. Cheung, G. L. Lin, Y. C. Lin, and H. L. Yu, Phys. Rev. D **46**, 1148 (1992); **55**, 5851(E) (1997).
[41] P. Colangelo, F. De Fazio, and T. N. Pham, Phys. Rev. D **69**, 054023 (2004).
[42] M. B. Voloshin, arXiv:1301.5068.
[43] Q. Wang, X.-H. Liu, and Q. Zhao, Phys. Rev. D **84**, 014007 (2011).
[44] Q. Wang, X.-H. Liu, and Q. Zhao, Phys. Lett. B **711**, 364 (2012).